Computational Engineering and Physical Modeling 4-1 (2021) 84-100

Contents lists available at **CEPM**

Computational Engineering and Physical Modeling

Journal homepage: www.jcepm.com

# Effect of Threshold Twin Volume Fraction in Crystal Plasticity Modeling

**F. Li, A. Chapuis*, Q. Liu**

College of Materials Science and Engineering, Chongqing University, 400044 Chongqing, China

Corresponding author: *achapuis@cqu.edu.cn*

https://doi.org/10.22115/CEPM.2021.245719.1128

**ARTICLE INFO**

Article history:
Received: 28 August 2020
Revised: 13 November 2020
Accepted: 05 January 2021

Keywords:
Twinning;
VPSC;
Magnesium.

**ABSTRACT**

Modeling of metals deforming by twinning requires reorienting the matrix into twin orientation. In twinning models like the Predominant Twin Reorientation scheme (PTR), a threshold volume fraction is defined with an empiric equation to reorient the parent grain into the dominant twin variant. This equation contains two parameters which are first investigated in the present study, showing their effect on simulated flow stress and twin volume fraction evolution. Magnesium, with a tension and a compression twinning modes, is taken as an example to compare the expected experimental behavior and the modeled behavior. Complex deformations such as strain path change and multiple twinning are modeled with the PTR, and simulated stress, twin volume fraction and texture are correlated with the expected behavior. The PTR shows a good agreement with experiments when the twin volume fraction corresponds to the fraction of grains reoriented into twins, but limited predictability when the twinned grains are not reoriented.

## 1. Introduction

Twinning is an important deformation mode in HCP metals such as Magnesium, Zinc, Titanium, and Zirconium [1]. Twinning is a common deformation mechanism that reorients a part of the

How to cite this article: Li F, Chapuis A, Liu Q. Effect of Threshold Twin Volume Fraction in Crystal Plasticity Modeling. Comput Eng Phys Model 2021;4(1):84–100. https://doi.org/10.22115/CEPM.2021.245719.1128

lattice (i.e. the parent grain) into a new orientation (i.e. the twin). Several twinning modes can be activated, particularly at low temperature. To model the plastic deformation behavior, such as flow stress and texture evolution, crystal plasticity based models must take twinning into account. The EPSC [2] and VPSC [3] initial versions include the predominant twin reorientation (PTR) scheme [4], in which a grain that deformed by twinning can be reoriented into the orientation of its most activated twin variant, so that the number of orientations is kept constant. Crystal plasticity finite element models (CP-FEM) that take into account twinning have to use an approach similar to the PTR for each element [5–8].

In the PTR, two parameters, $A^{th1}$ and $A^{th2}$, regulate the twinning events in an equation. Note that reorientation could also be dictated by one equation using a single parameter [9]. The twinning-detwinning (TDT) model [10] has been developed to take into account all the twin variants. In the TDT, the parent grain and all twin variants are represented by a grain with its own volume fraction and orientation. In both the PTR and the TDT, the twinning events are controlled by a threshold twin volume fraction. In the PTR, the threshold twin volume fraction controls the number of parent grains that can be reoriented into twin orientations at each deformation step, while in the TDT model, it prevents deformation by twinning in the parent grains. Although the TDT model allows much better texture predictions than the PTR [11], the TDT is not adapted to model multiple twinning events, such as double twinning $\{10\bar{1}1\}$-$\{10\bar{1}2\}$ or secondary twinning $\{10\bar{1}2\}$-$\{10\bar{1}2\}$ that may happen during strain path change [12].

In magnesium and its alloys, $\{10\bar{1}2\}$ tension twinning is one of the main deformation mode, and its activation highly depends on the strain path. Generally, $\{10\bar{1}2\}$ twinning is initiated by a tensile stress parallel to the lattice <c> axis (for example by tension along the normal direction (ND) of a rolled plate), or a compressive stress perpendicular to the <c> axis (for example by in-plane compression along the rolling direction (RD) or the transverse direction (TD) of a rolled plate). The flow stress of $\{10\bar{1}2\}$ twinning-predominant deformation is characterized by an S-shaped curve, because twinning is easy but twins have a hard orientation. The activated twin variants mainly follow the Schmid law [13–15]. Tension twins reorient the lattice at about $86^{o}$, and the most favorable twin variant is oriented with <c> close to the compression direction.

Although the equation of the threshold twin volume fraction can be adjusted to fit the S-shaped flow curve of $\{10\bar{1}2\}$ twinning predominant deformation, its parameters have no physical meaning, resulting that stress increase is artificially controlled. The value of the 2 parameters controlling the threshold twin volume fraction depends on the twinning mode. For tension twinning in magnesium, the values $A^{th1}$ and $A^{th2}$ are high, in order to reproduce the stress plateau and slow hardening during twinning. But for $\{10\bar{1}1\}$ twinning, the value are low in order to model the softening induced by compression twins [11,16].

Up to now, there are no detailed study investigating the effect of PTR parameters on the reproducibility of the deformation behavior, and in particular on the flow stress and texture evolution. This study aims to fill this gap and to investigate whether suitable parameters can allow to reproduce some complex twinning events.

## 2. Experimental procedure

### 2.1. Modeling background

For this study, the numerical simulations are effected by the visco-plastic self-consistent (VPSC) model of Lebensohn and Tomé [3]. The model is applied to magnesium, but results can be extrapolated to other HCP materials undergoing extensive twinning. For Mg alloys, basal <a> ($\{0001\}\langle 11\bar{2}0\rangle$), prismatic <a> ($\{10\bar{1}0\}\langle 11\bar{2}0\rangle$), and pyramidal <c+a> ($\{10\bar{1}1\}\langle \bar{1}\bar{1}23\rangle$) slip are considered, as well as $\{10\bar{1}2\}\langle \bar{1}011\rangle$ tension twinning and $\{10\bar{1}1\}\langle 10\bar{1}\bar{2}\rangle$ compression twinning.

For both slip and twinning, the resolved shear stress, $\tau^{\alpha}$, is the driving force for the shear rate, $\dot{\gamma}^{\alpha}$; and slip obeys the rate sensitive equation (1),

$$\dot{\gamma}^{\alpha} = \dot{\gamma}_0 \left(\frac{|P^{\alpha}:\sigma|}{\tau_c^{\alpha}}\right)^n sgn(P^{\alpha}:\sigma) \tag{1}$$

Where $P^{\alpha}$ is the Schmid tensor, $\dot{\gamma}_0 = 1s^{-1}$ is a reference shear rate, $\tau^{\alpha} = P^{\alpha}:\sigma$ is the resolved shear stress, $\tau_c^{\alpha}$ is the critical resolved shear stress (CRSS) and $m$ =1/$n$=0.05 is the strain-rate sensitivity parameter.

Twinning follows the equation:

$$\dot{\gamma}^{\alpha} = \begin{cases} \dot{\gamma}_0 \left|\frac{\tau^{\alpha}}{\tau_c^{\alpha}}\right|^{\frac{1}{m}} & \tau^{\alpha} > 0 \\ 0 & \tau^{\alpha} < 0 \end{cases} \tag{2}$$

To model twinning, the predominant twin reorientation scheme (PTR) is used [4]. In the PTR approach, within each grain $g$ the program keeps in memory the shear strain $\gamma^{t,g}$ contributed by each twin system $t$, and the associated volume fraction $V^{t,g}$=$\gamma^{t,g}/S^t$ ($S^t$ is the characteristic twin shear of the twinning mode). The sum over all twin systems of a twin mode, and over all grains, represents the 'accumulated twin fraction' $V^{acc,mode}$ in the aggregate for the twin mode (it is the volume fraction that can be measured by EBSD).

$$V^{acc,mode} = \sum_g \sum_t \gamma^{t,g}/_{S^t} \tag{3}$$

In order to keep the number of grains constant, the PTR scheme adopts a statistical approach. At each step increment, some grains are fully reoriented into twin if the following condition is met. The volume associated with the fully reoriented grains for that mode is called 'effective twinned fraction' $V^{eff,mode}$, and a threshold volume fraction is defined as:

$$V^{th,mode} = \min\left(1,\ A^{th1} + A^{th2}\frac{V^{eff,mode}}{V^{acc,mode}}\right) \tag{4}$$

$A^{th1}$ and $A^{th2}$ are the two artificial material constants whose effect will be investigated in the present study. After each deformation step a grain is randomly picked and the twin system with

the highest accumulated volume fraction is identified. If the latter is larger than the threshold $V^{th,mode}$ then the grain is reoriented into that twin orientation and $V^{eff,mode}$ and $V^{th,mode}$ are updated. The random process is repeated until either all grains are checked or until the effective twin volume fraction exceeds the accumulated twin volume fraction. Then the program stops reorientation by twinning and continues to the next deformation step. This process results in two things: a) only the historically most active twin system in each grain is considered for reorienting the grain into twin; b) the twinned fraction is consistent with the shear activity that the twins contribute to deformation. The algorithm controlled by equation (4) prevents grain reorientation by twinning before that a threshold value $A^{th1}$ is accumulated in any twinning system (typically 10-30% volume fraction) and rapidly increases the threshold to a value around $A^{th1} + A^{th2}$ (typically 50-80% volume fraction).

The response of a polycrystal material is obtained by applying the self-consistent approach. Several linearization schemes have been proposed, and in the present study the *Affine* self-consistent scheme is used. The *Affine* formulation was found to reproduce better the experimental behavior of magnesium alloys [17].

**Table 1**
Material parameters inputs for the VPSC-PTR model.

| Mode | basal | prismatic | <c+a> | $\{10\bar{1}2\}$ | $\{10\bar{1}1\}$ |
|---|---|---|---|---|---|
| $\boldsymbol{\tau_0 = \tau_c}$ (MPa) | 20 | 120 | 160 | 25 | 140* |

* If considered.

The material parameters (i.e., the CRSS) used in the present study are given in Table 1, and are inspired by the CRSS determined for Mg alloy AZ31 [11]. The CRSS are kept constant so that the flow stress depends solely on the texture. Whether compression twinning $\{10\bar{1}1\}$ is considered will be specified in each section.

## 2.2. Material and experiments

The material used for both experiments and simulations is a hot rolled and annealed 2h at 400ºC AZ31 alloy with a strong basal texture, with most c-axis almost parallel to the normal direction. The initial texture, discretized into 1000 grain orientations of equal volume fraction for simulations, is shown in figure 1. The initial texture was measured by EBSD.

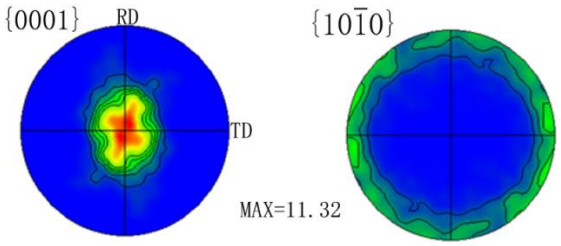


**Fig. 1.** Initial texture of hot rolled AZ31.

Some samples RD10*TD8*ND7 mm were cut in the hot rolled plate and annealed. Compression was performed at 0.001 $s^{-1}$ on a SHIMADZU AG-X50kN. Teflon and graphite were used as

lubricant in order to minimize friction and barreling. Then the deformed samples were cut in two in a plane containing the loading direction, and the surface was manually polished by carbon paper from 1000# to 4000#, and the commercial AC2 solution was used to final electro-polishing. The voltage and current were 20V and about 0.05A, respectively. EBSD was performed on TESCAN VEGA. The accelerating voltage was 20kV, step size was 1μm and the scanned area was about 300*300μm.

## 3. Simulated results

### 3.1. Monotonic twin dominated deformation

In order to investigate the effect of the parameters $A^{th1}$ and $A^{th2}$, the VPSC model with PTR was used to simulate the plastic deformation during uniaxial loading. Both crystallographic slip and deformation twinning participate to the deformation and texture evolution. The lattice re-orientation induced by deformation twinning is dictated by the PTR scheme described previously. Only slip and $\{10\bar{1}2\}$ tension twinning are considered in this section, and RD compression is modeled as a case example.

Figure 2 shows for different $A^{th1}$ (Fig.2a-b) and different $A^{th2}$ (Fig.2c-d) the simulated flow stress (Fig.2a-c), accumulated twinned volume fraction (TVF) $V^{acc}$ and effective TVF $V^{eff}$ (Fig.2b-d). As expected, $V^{acc}$ is always bigger than or equal to $V^{eff}$. The flow stress follows the same tendency as $V^{eff}$, which means the texture rotation by slip is negligible compare to the texture re-orientation by $\{10\bar{1}2\}$ twinning. $A^{th1}$ determines the strain at which grains start to be re-oriented into twins, and so the flow stress starts to increase. $A^{th2}$ determines how quickly the threshold volume fraction increases, with low value $A^{th2}$ provoking a fast increase of $V^{eff}$ and of the flow stress, because of a slow increase of the threshold. Consequently, $A^{th2}$ determines the hardening rate associated with twinning exhaustion and the beginning of the deformation of twins. In other words, the higher are $A^{th1}$ and $A^{th2}$, the more delayed is the grain re-orientation into twin. The accumulated twin volume fraction increases linearly and independently of $A^{th1}$ and $A^{th2}$ at low strain, but at high strain it should be equal to $V^{eff}$. The figure 2 also shows that the flow stress continues to increase slightly after all favorable grains are reoriented, that is to say when the $V^{eff}$ saturates. Major differences between $V^{acc}$ and $V^{eff}$ are observed when $V^{acc}+V^{eff}\geq 1$. The flow stress increase at high strain is due to grain rotation by slip toward harder orientations. $V^{eff}$ saturates at ~80%, obviously about 20% of the grains of the initial texture are not favorably oriented for tension twinning during this strain path. $A^{th1}$ and $A^{th2}$ influence the maximum twin volume fraction: because grains already reoriented into twins do not deform by $\{10\bar{1}2\}$ twinning anymore, low $A^{th1}$ and $A^{th2}$ tends to decrease the $V^{acc}$. But high $A^{th1}$ and $A^{th2}$ (i.e. close to 1 or higher) tend to prevent grain reorientation into twins, resulting in slightly lower $V^{eff}$ but much higher $V^{acc}$. Actually, at high strain $A^{th1}$ and $A^{th2}$ hardly affect the effective twin volume fraction and the flow stress.

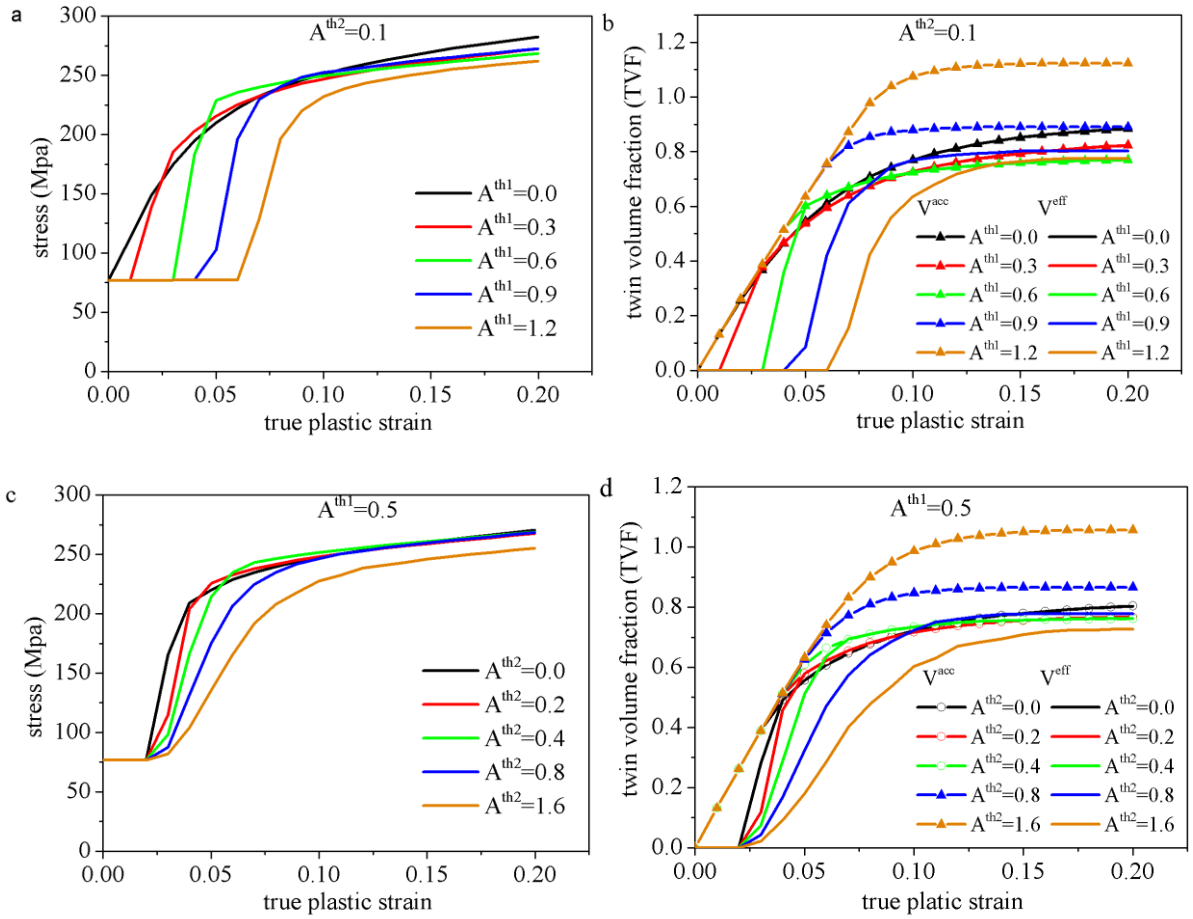


**Fig. 2**. VPSC simulation of RD compression (a) flow stress with different $A^{th1}$ and $A^{th2}$=0.1; (b) corresponding accumulated and effective TVF, (c) flow stress with $A^{th1}$=0.5 and different $A^{th2}$ and (d) corresponding TVF.

Experimentally, at low strain, the tension twin fraction is proportional to the strain; so that twinning occurs at the yield point as has been confirmed by acoustic emission and digital-image correlation experiments [18]. Heterogeneous deformation happens during yielding, and twins easily propagate from grain to grain, resulting in 'cross-boundary twins', and a 'Lüders-like yield elongation' is observed [19,20]. Consequently, some sample-areas are free of twins, whereas some other areas are full of 'cross-boundary twins'. During plastic deformation, $\{10\bar{1}2\}$ twinning generate grain subdivision, lattice reorientation, and accommodation of strain along the <c> axis [13,21–23]. If one wants to fit the texture evolution, it will be judicious to choose low values $A^{th1}$ and $A^{th2}$, mainly at low strain. If one wants to fit the stress-strain curves, generally high values $A^{th1}$ and $A^{th2}$ are required [24].

## 3.2. Strain path change

Forming operations often produce severe strain path changes which modeling is challenging. In order to investigate whether the PTR can reproduce both the expected flow stress and the texture during a complex strain path change, several experiments and simulations are presented in this section. Pre-compression along RD to ε=3% and subsequent compression along TD is shown in

figure 3a; the texture evolution has been tracked by EBSD. Primary $\{10\bar{1}2\}$ tension twins are formed during the RD pre-compression, and generate the texture component with <c> close to RD (hereafter simply denoted <c>//RD). After TD compression, in grains already twinned both new twins and secondary twins $\{10\bar{1}2\}$-$\{10\bar{1}2\}$ will appear in the matrix and in the primary twins, respectively. These new twins result in the formation of the texture component <c>// TD, while the intensity of the components <c>//ND and <c>//RD decreases progressively.

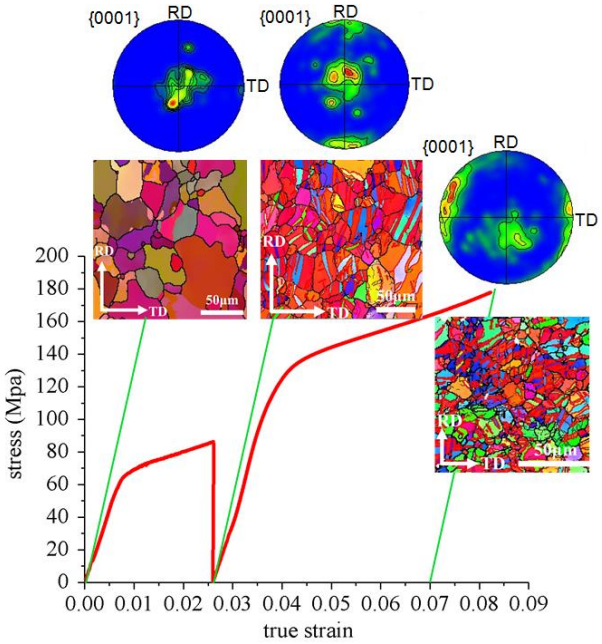


**Fig. 3.** Experimental flow stress and texture evolution during RDc3-TDc5.

For simplicity in this section, simulations were executed considering only slip and tension twinning with $A^{th1}$=0.7 and $A^{th2}$=0.1. Several pre-compression strains along RD are modeled: 3, 5 and 10%; followed by TD compression. The total deformation path will be called thereafter RDc3TDc, RDc5TDc and RDc10TDc, respectively. Simulated results, showing the stress strain curves, the twin volume fraction evolutions, and the textures, are shown in figures 4. It is important to note that a complex strain path can be input for the simulations, so not only the texture but also the activity and twin volume fraction of each variant are kept into memory at the beginning of the second deformation.

For the 3 cases examined, the yield stress at re-loading is relatively low and corresponds to twin dominated deformation. The sharp increases of flow stress are correlated with sharp increases of the effective twin volume fraction $V^{eff}$. Meanwhile, $V^{eff}$ has similar trend in the three cases: no twins below 3% strain, a rapid increase with further strain (whatever strain is along RD or TD), and then slower increase, which is even a plateau in RDc10TDc, a second sharp increase after about 4% of TD compression, and a final saturation. The maximum TVF is the highest for RDc10TDc, and the lowest for RDc3TDc. The figures 4b-c-d show the relationship between the effective twin volume fraction ($V^{eff}$) and the corresponding texture at different strains. After the last twinning events, the texture is similar in the three samples, with <c> close to TD (<c>//TD) and a total disappearance of the texture components <c> close to RD and ND. The texture is

unchanged after 3% RD compression, because of the high value of $A^{th}$ .For a pre-strain 3% (Fig. 4b), between 3 to 5%, the predicted texture evolution shows an unreliable trend: a <c>//RD component appears. This is because the VPSC kept in memory a high volume fraction of twin variants activated during RDc, and so reorient the grain into these variants during re-loading. This behavior can be understand reminding that the twin volume fraction is tracked during the whole deformation. After RDc3%, in some grains favorably oriented, the most activated twin variant accounted for about 50%, such grains will be reoriented with <c> close to RD even if other variants are activated during TD compression. Then, between 8 to 9% strain this grains oriented <c>//RD undergo secondary twinning and the texture <c>//TD predominates.

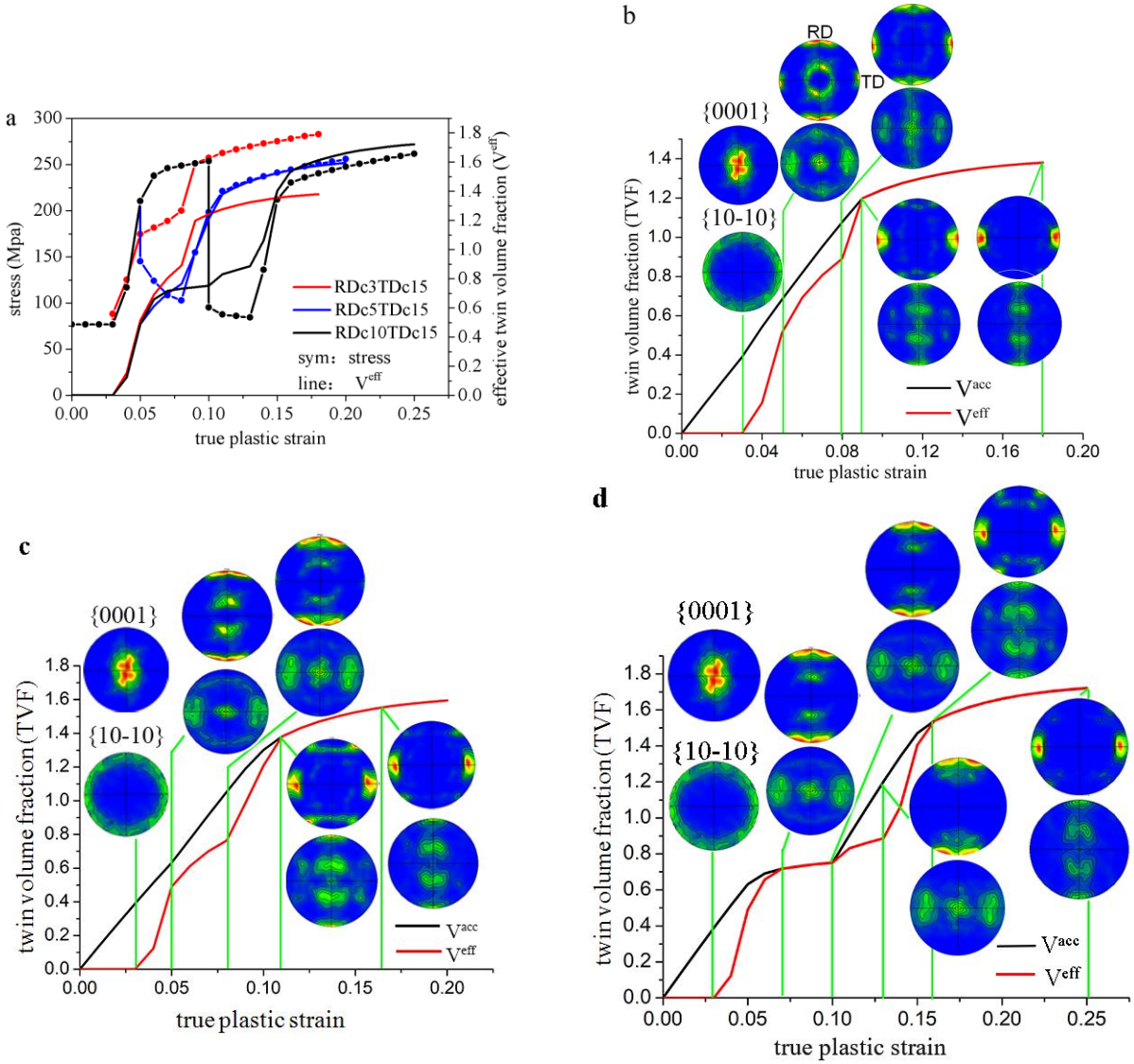


**Fig. 4.** (a) Flow stress (symbols) and effective twin volume fraction (line), texture development and twin volume fraction (accumulated and effective) *vs* strain corresponding to (b) RDC3TDC15, (c) RDC5TDC15, and (d) RDC10TDC15.

When the pre-strain is 5% (fig. 4c), the <c>//RD component is created before ε=5%, but strengthen until ε=8%: similarly as in RDc3TDc, some grains had a high volume fraction of

twins with <c>//RD but have not been reoriented during the pre-compression, so they reorient when their total twin volume fraction increased (i.e. during TDc), but reorient into the predominant variant <c>//RD. After that, as TD compression continue, these re-oriented grains can twin again and will lately re-orient into <c>//TD.

The texture evolution for the RDc10TDc (fig 4d) corresponds to what is expected, with twins with <c> close to RD after pre-compression that deform by secondary twinning during TD compression; except that between 10% and 13% total strain some grains, whose parent orientation was tilted between ND and RD, seem to be re-oriented close to RD. During the TD compression, reoriented grains re-twin and re-orient when their twin volume fraction is high enough (at about $V^{acc}=A^{th1}+A^{th2}=0.8$).

We can extrapolate that during RDc1TDc, the twin volume fraction of the most favorable variant would be much less than 50%, and so all grains will be reoriented into twins with <c>//TD directly.

## 3.3. Detwinning

Figure 5 shows an example of strain path change promoting twinning and detwinning: pre-compression along RD to ε≈3% followed by ND compression. Because the sample sides were not parallel anymore, the experimental flow stress at reloading is not reliable and we cannot see at what flow stress detwinning happens. The texture change is however obvious and the <c>//RD component disappeared after ND compression to ε≈3%.

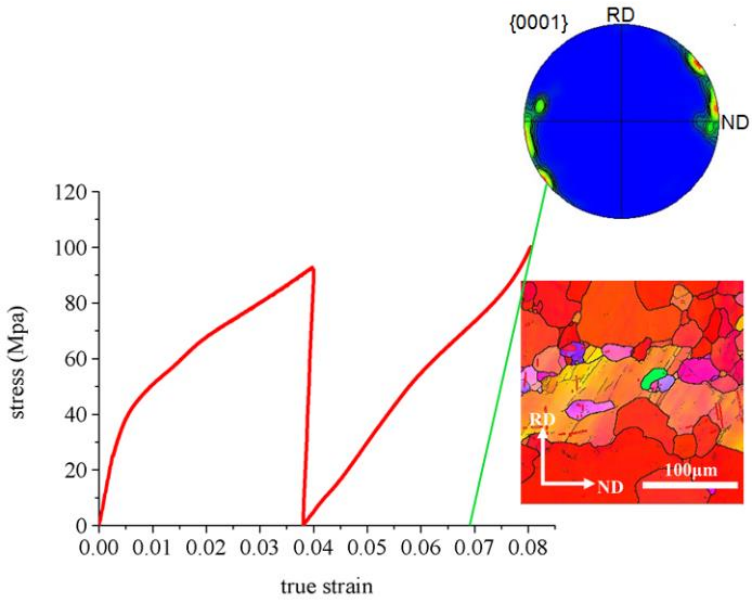


**Fig. 5**. stress-strain curve and texture after RDc3-NDc3.

When the strain path change provokes a migration of the twin boundary fraction so that the twin volume fraction decreases and the parent grain fraction increases, detwinning happens. Tension twins in magnesium are easily subject to detwinning, which has been considered to happen at lower stress than twin nucleation [25], but simulation studies conducted with the elasto-visco-plastic self-consistent model with twining de-twining scheme (EVPSC-TDT) have shown that

the driving force for twinning and detwinning are similar, i.e., the CRSS is the same [26]. Whether the driving force has to be applied to the twin or the matrix is undefined, however in the TDT model, twin growth or twin shrinkage are modeled to happen in both the matrix and the twin. When the deformation is modeled, often all the twin variants have the same CRSS, so inside the twin a variant close to the matrix orientation may be activated instead of the variant corresponding to the matrix, so the simulated texture may change a little. It is important to note that in the VPSC-PTR, twin shrinkage cannot happen in not re-oriented parent grains, even if the twin volume fraction is positive. In this section, two strain path changes will be considered: first RD compression followed by ND compression; second RD compression followed by RD tension. Note that the second correspond to reverse loading. Once again, compression twinning is not considered (inactive).

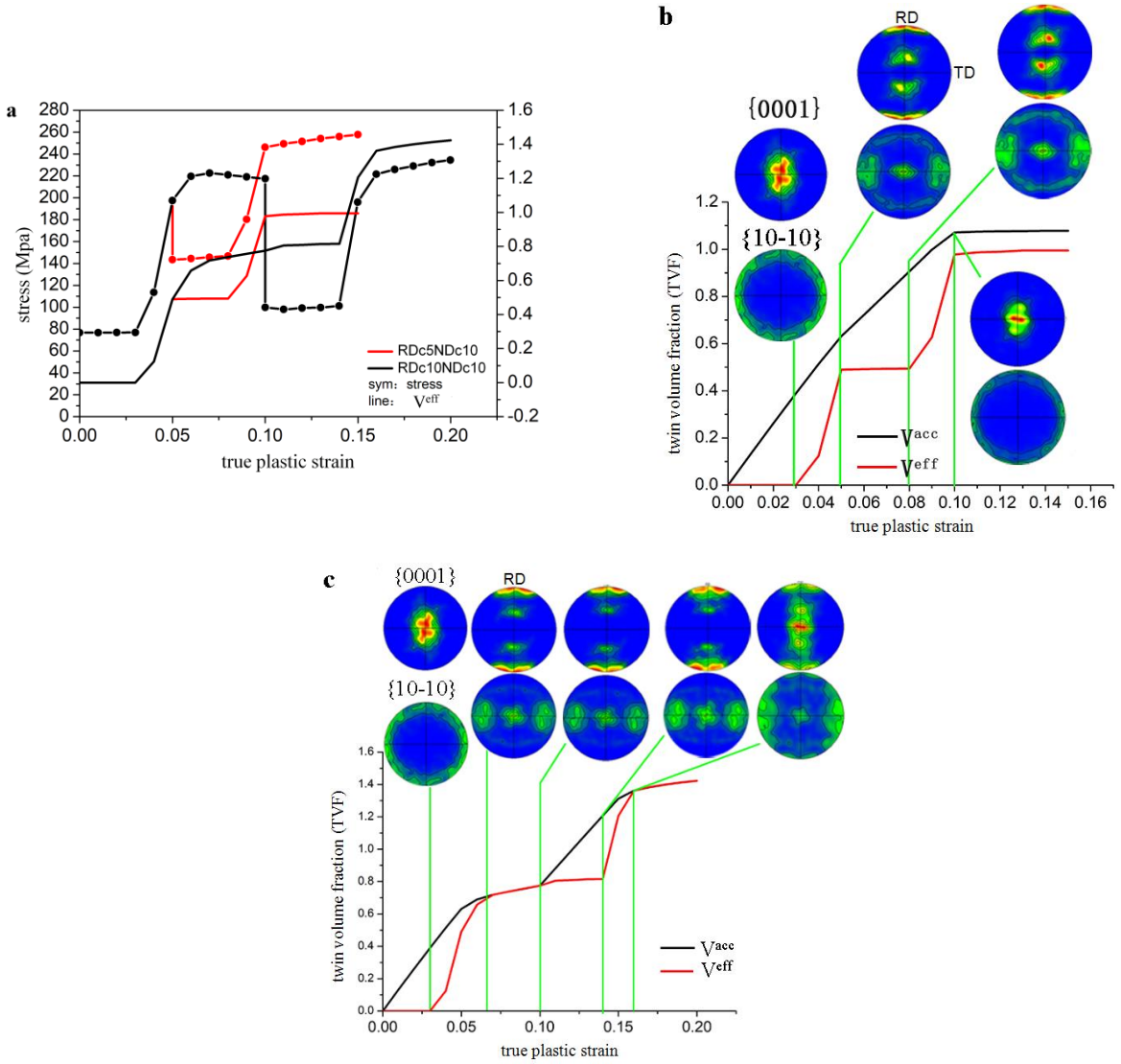


**Fig. 6**. (a) Flow stress (symbols) combined with effective twin volume fraction (line); texture evolution combined with accumulated and effective twin volume fractions for (b) RDc5-NDC and (c) RDc10NDc.

Figure 6 shows the simulated flow stress, twin volume fractions ($V^{eff}$ and $V^{acc}$), and predicted texture evolution during RD pre-compression to different strain followed by ND compression. Again, $A^{th1}$=0.7 and $A^{th2}$=0.1 in all this section. When RD pre-compression is less or equal 5%, only a fraction of the grains deforming by twinning are re-oriented, and $V^{eff}<V^{acc}$. As ND compression proceed, the total $V^{acc}$ continues to increase, but only grains re-oriented into twins can re-twin and be re-oriented into <c> close to ND. In RDc10NDc, most (80%) of the original grains are re-oriented into twins and $V^{acc}=V^{eff}$ after RD pre-compression, so during the subsequent ND compression all re-oriented grains close to RD should deform by twinning and reorient into orientations <c>//ND. Whether this secondary twin variant corresponds to the orientation of the initial matrix cannot be ascertain, because slip occurred in both matrix and twin, so the final texture cannot be exactly the initial one. But in compression 1 or 2 twin variants have a Schmid factor much higher than the other, so the variant activated during ND recompression is likely to correspond to the matrix, or is close to its orientation. Moreover, it can be seen that a very few grains re-orient at the beginning of ND compression (certainly into orientations <c> close to RD). The twin volume fraction continues to increase beyond 10% ND compression, certainly due to the component <c> close to RD that remains even after a total strain ε=20%. Considering the phenomenon observed during strain path change in section 3.2, such un-reoriented parent grains were wrongly reoriented into <c>//RD during ND compression. Another observation is that when $V^{acc}=V^{eff}$, the threshold is high, so grains are slowly reoriented, whereas when $V^{acc}>V^{eff}$, such as in RDc5NDc, the reorientation by secondary twinning (or detwinning) is achieved at relatively low strain (5% NDc). In summary, detwinning can be better modeled when $0<V^{eff}<V^{acc}$, but the texture is reliable when $V^{eff}=V^{acc}$.

Reverse loading and detwinning are illustrated by RD compression followed by RD tension in figure 7. When RD pre-compression is 3% (RDc3RDt), no grains are re-oriented into twins during the pre-compression, so the behavior is the same as if tension was directly applied. A few grains, whose orientation is certainly far from the basal texture, deform by twinning and are re-oriented during tension. After RD tension, the distribution of the basal pole is unchanged, but $\{10\bar{1}0\}$ aligns with the tensile direction, due to prismatic slip [27]. When RD pre-compression is 5 or 10%, some grains are re-oriented into twins with c//RD. During the subsequent tension, these grains deform by twinning. Theoretically, the 6 variants should be almost equally activated during RD tension, so the secondary twins should spread in the ND-TD plane, as was observed during ND tension in [11]. But clearly one variant has an advantage, and it corresponds to the orientation of the initial matrix, so the initial texture is almost recovered. Because of slip that happened in RDc10, the texture after RDc10RDc10 results from the selection of a twin variant that may be different than the matrix and <c> spreads a little in ND-TD plane. In RDc5RDt detwinning is complete after 5% tension, whereas in RDc10RDt detwinning is achieved only after 10% tension. Once again, simulated results are closer to experimental expectation when $0<V^{eff}<V^{acc}$.

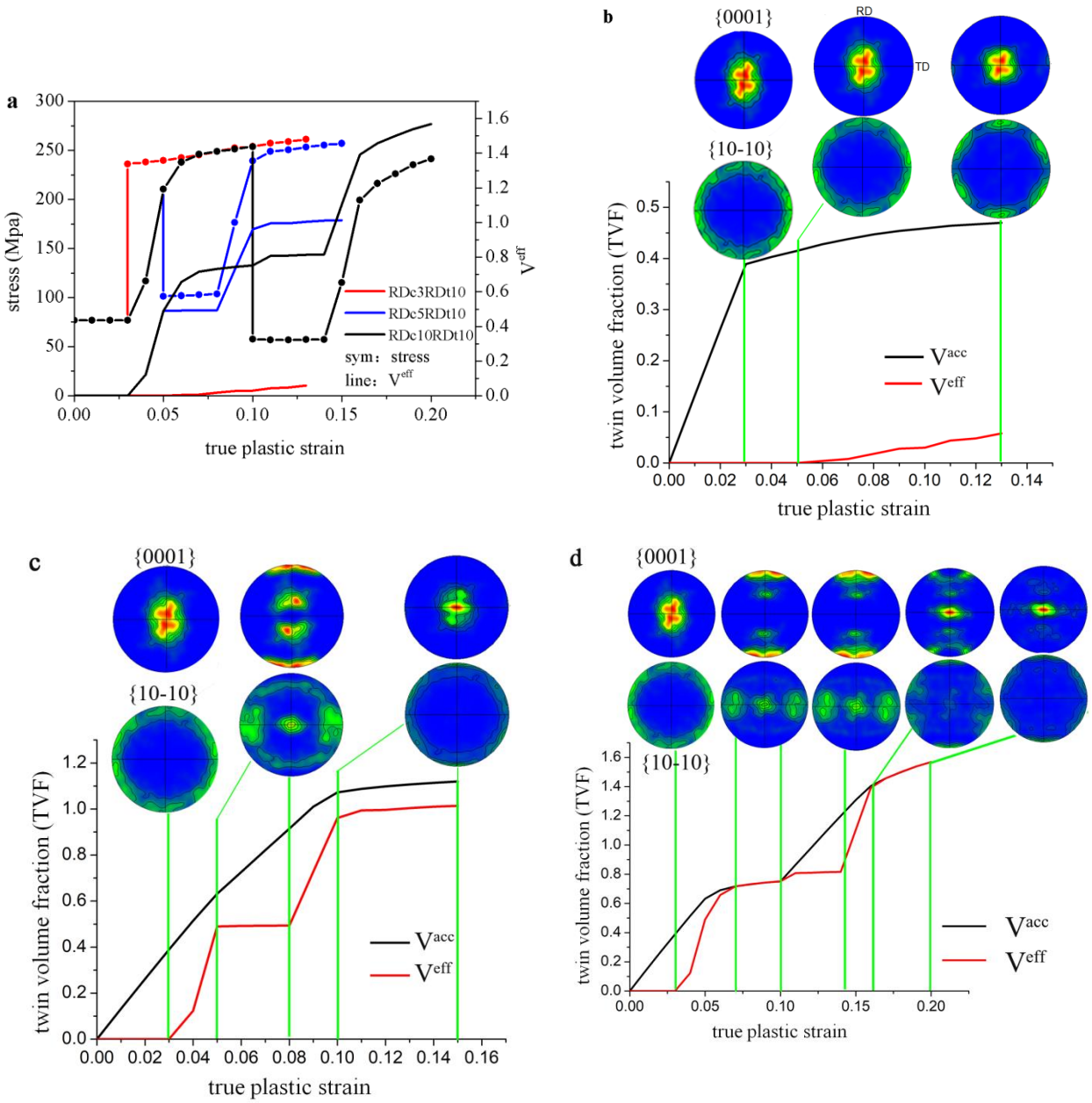


**Fig. 7.** (a) Flow stress and effective twin volume fraction (TVF), texture evolution combined with accumulated and effective twin volume fraction in (b) RDc3RDt10, (c) RDc5RDt10 and (d) RDc10RDt10.

## 3.4. Double and tertiary twinning

During <c> axis compression, typically during ND compression, $\{10\bar{1}1\}$ twins are observed at relatively high strain (~5%) and immediately endure a subsequent $\{10\bar{1}2\}$ twin, forming the well-known double twins $\{10\bar{1}1\}$-$\{10\bar{1}2\}$, which are generally misoriented 38º with the parent lattice [28,29]. It is important to note that such double twins are not predicted correctly by self-consistent models [23]: contraction twins can deform easily by basal slip or another tension twin variant may be predicted. Only CPFEM can predict the occurrence of the observed twin variant

[23]. During in-plane compression, tension twins reorient totally the texture, and then compression twinning happens, so that tertiary twins {10-12}-{10-11}-{10-12} are observed above ~10% strain [30]. The VPSC-PTR can allow or prevent grains to undergo multiple twinning events: as previously secondary twinning is allowed.

In this section, $\{10\bar{1}1\}$ compression twinning is considered ($\tau_c^{\{10\bar{1}1\}}$=140 MPa, $A^{th1}$=0.1 and $A^{th2}$=0.1) in addition to the other deformation modes. ND compression is simulated, and the simulated results are shown in figures 8.

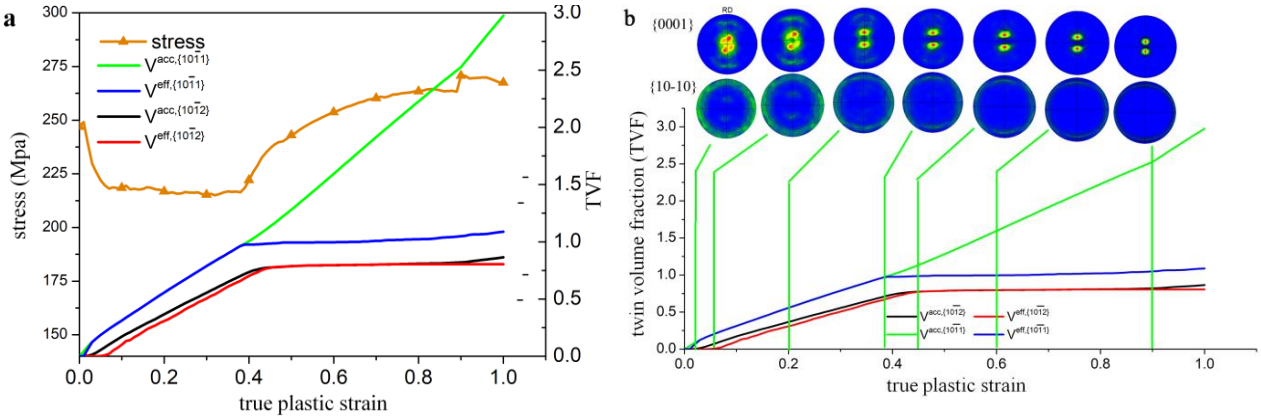


**Fig. 8**. simulated ND compression (a) flow stress, $\{10\bar{1}2\}$ tensile twin and $\{10\bar{1}1\}$ compression twin volume fractions, (b) texture evolution and TVF *vs* true plastic strain.

During ND compression simulations, $\{10\bar{1}1\}$ compression twinning is first activated, and grains start to be re-oriented into compression twins after ~1% strain, due to the low $V^{th}$. After ε=5% some grains, certainly some primary compression twins, start to be re-oriented into $\{10\bar{1}2\}$ twins. Compression twins are misoriented 64° with the matrix, and generate the two texture components with <c> tilted ~50° between ND and RD. Double twins do not generate another new texture component, but are slightly tilted between ND and RD, so that a (0001) texture with a double peaks close to ND slightly tilted toward RD is quickly generated and persists. According to simulation results, both the $\{10\bar{1}1\}$ and $\{10\bar{1}2\}$ twin volume fractions continuously increase until ε≈0.4. Because $V^{acc,\{10\bar{1}1\}}$ continuously increases, it is clear that the $\{10\bar{1}1\}$-$\{10\bar{1}2\}$ twins deform by compression twinning. It seems that during the deformation, all grains are re-oriented into compression twins, and then re-oriented into tension twins, but further multiple twinning events (i.e. reorientations) are forbidden. Secondary twinning is allowed in the program; however tertiary twinning is considered as a deformation mode but does not result as a grain reorientation.

It can be extrapolated (results not shown for simplicity) that $\{10\bar{1}2\}$-$\{10\bar{1}1\}$-$\{10\bar{1}2\}$ tertiary twinning which is expected to occurs during TD or other in-plane compression cannot be modeled: grains re-orient into $\{10\bar{1}2\}$ twins, then into $\{10\bar{1}2\}$-$\{10\bar{1}1\}$, and then even if $V^{acc,\{10\bar{1}2\}}$ and $V^{acc,\{10\bar{1}1\}}$ increase, no further re-orientation can happen.

## 4. Discussion

The parameters controlling the threshold twin volume fraction $A^{th1}$ and $A^{th2}$ are generally fixed to reproduce the S-shape of the stress strain curve, but they should be physically connected: if twins are harder than the matrix and do not deform by slip until twinning exhaustion, such as tension twins in Mg, the value $A^{th1}$ should be high. If twins are softer than the matrix and deform, such as compression twins, the value $A^{th1}$ should be low. But the right texture can be reproduced by the simulations only when the accumulated twin volume fraction $V^{acc}$ is equal to the effective TVF $V^{eff}$. The section 3.1 has shown that $V^{acc}=V^{eff}$ after a critical strain or after twinning exhaustion if $0<A^{th1}+A^{th2}<1$. Only the TDT model can reproduce both the flow stress and the texture evolution during tension twin dominated deformation [11]. The TDT model has been developped mainly to simulate twinning followed by detwinning [10]. Recently, secondary twinning was included in a modified version of the TDT model [12], but a PTR approach was necessary for the secondary twins to avoid dealing with too many secondary twin variants and an extended computation time.

The previous simulated results, compared with what is expected based on experimental results, show that the PTR can actually predict the expected texture in some cases, but fails under certain conditions. In particular, the PTR can predict the expected texture in the following cases:

-When $V^{eff}=V^{acc}$ and there is no grain with a total twin volume fraction higher than 50% but not reoriented into twins. This has been shown by strain path change simulations; for example RDc5-TDc contained some grains un-reoriented after RD compression but with a high twin volume fraction, resulting in a wrong texture evolution during the subsequent TD compression. On the opposite in RDc10-TDc twinned grains were all reoriented so the texture was well predicted. Detwinning could also be reasonably simulated provided that the same conditions are fulfilled.

-At high strain, but only when 1 variant largely predominates on the others, such as in compression. Simulations with the TDT model have shown that during TD compression the predominant twin variant (with the highest Schmid factor) accounts for 60% of the twinning, and the second most active variant accounts for only 30% [11].

-At high strain after a strain path change, when grains, even with complex twinning history, are re-oriented toward their final orientation.

On the opposite, the VPSC-PTR fails to predict the expected texture evolution in the following cases:

-At low strain, when $V^{eff}<V^{acc}$, that is to say before enough grains with twins be re-oriented into twins. This problem can be solved by fixing adequately $A^{th1}$ and $A^{th2}$.

-During strain path change, when some grains have a high twin volume fraction but have not been re-oriented. They later re-orient into the ‘wrong’ twin variant. This problem was shown during RDc3-TDc and RDc5-TDc.

- In tension along ND or along the <c> axis of the grains, it has been shown [11] that the most activated twin variant represented only 25% of the twins; and the other variants were well

represented. This resulted in a fiber texture with <c> perpendicular to ND, well predicted by the TDT model, whereas the PTR predicted a nearly basal texture with <c>//RD.

## 5. Conclusion

The VPSC-PTR was used to simulate the flow stress and texture change associated with twinning. Experiments were made to show and understand the expected texture evolution. The following conclusions were reached:

1. The parameters controlling the threshold twin volume fraction $A^{th1}$ and $A^{th2}$ both delay re-orientation into twin, so that high values allows more twinning to occur without texture change. In the case of tension twinning, high $A^{th1}$ and $A^{th2}$ also delay the flow stress increase.

2. Secondary twinning, double twinning and detwinning may be reproduced with the inaccuracy and low computational cost permitted by the PTR.

3. Texture can be simulated successfully during a strain path change, but only if highly twinned grains were reoriented into twins at reloading and when the texture is simulated.

4. The behavior during detwinning can also be reproduced if enough grains were allowed to re-orient before the reverse loading.

5. The PTR can better reproduce the texture in compression than in tension, because in tension along the <c> axis all variants are equally stressed.

## Acknowledgements

Thanks go to C.N. Tomé for sharing the VPSC code. Discussion with P.D. Wu motivated this study. F.Y. Li is supported by the National Natural Science Foundation of China (51421001), and the '111' Project (B16007) by the Ministry of Education and the State Administration of Foreign Experts Affairs of China.

## References

[1] Partridge PG. The crystallography and deformation modes of hexagonal close-packed metals. Metall Rev 1967;12:169–94. doi:10.1179/mtlr.1967.12.1.169.

[2] Turner PA, Tomé CN. A study of residual stresses in Zircaloy-2 with rod texture. Acta Metall Mater 1994;42:4143–53. doi:10.1016/0956-7151(94)90191-0.

[3] Lebensohn RA, Tomé CN. A self-consistent anisotropic approach for the simulation of plastic deformation and texture development of polycrystals: Application to zirconium alloys. Acta Metall Mater 1993;41:2611–24. doi:10.1016/0956-7151(93)90130-K.

[4] Tomé CN, Lebensohn RA, Kocks UF. A model for texture development dominated by deformation twinning: Application to zirconium alloys. Acta Metall Mater 1991;39:2667–80. doi:10.1016/0956-7151(91)90083-D.

[5] CHOI S, SHIN E, SEONG B. Simulation of deformation twins and deformation texture in an AZ31 Mg alloy under uniaxial compression. Acta Mater 2007;55:4181–92. doi:10.1016/j.actamat.2007.03.015.

[6] Choi S-H, Kim DH, Lee HW, Shin EJ. Simulation of texture evolution and macroscopic properties in Mg alloys using the crystal plasticity finite element method. Mater Sci Eng A 2010;527:1151–9. doi:10.1016/j.msea.2009.09.055.

[7] Abdolvand H, Daymond MR. Internal strain and texture development during twinning: Comparing neutron diffraction measurements with crystal plasticity finite-element approaches. Acta Mater 2012;60:2240–8. doi:10.1016/j.actamat.2012.01.016.

[8] Qiao H, Barnett MR, Wu PD. Modeling of twin formation, propagation and growth in a Mg single crystal based on crystal plasticity finite element method. Int J Plast 2016;86:70–92. doi:10.1016/j.ijplas.2016.08.002.

[9] Qiao H, Wu PD, Guo XQ, Agnew SR. A new empirical equation for termination of twinning in magnesium alloys. Scr Mater 2016;120:71–5. doi:10.1016/j.scriptamat.2016.04.015.

[10] Wang H, Wu PD, Wang J, Tomé CN. A crystal plasticity model for hexagonal close packed (HCP) crystals including twinning and de-twinning mechanisms. Int J Plast 2013;49:36–52. doi:10.1016/j.ijplas.2013.02.016.

[11] Zhao L, Guo X, Chapuis A, Xin Y, Liu Q, Wu P. Strain-Path Dependence of $$ \{ 10\bar{1}2\} $$ { 10 1 ¯ 2 } Twinning in a Rolled Mg–3Al–1Zn Alloy: Influence of Twinning Model. Metall Mater Trans A 2019;50:118–31. doi:10.1007/s11661-018-4955-y.

[12] Qiao H, Guo XQ, Hong SG, Wu PD. Modeling of {10-12}-{10-12} secondary twinning in pre-compressed Mg alloy AZ31. J Alloys Compd 2017;725:96–107. doi:10.1016/j.jallcom.2017.07.133.

[13] Brown DW, Agnew SR, Bourke MAM, Holden TM, Vogel SC, Tomé CN. Internal strain and texture evolution during deformation twinning in magnesium. Mater Sci Eng A 2005;399:1–12. doi:10.1016/j.msea.2005.02.016.

[14] Pei Y, Godfrey A, Jiang J, Zhang YB, Liu W, Liu Q. Extension twin variant selection during uniaxial compression of a magnesium alloy. Mater Sci Eng A 2012;550:138–45. doi:10.1016/j.msea.2012.04.046.

[15] Wang B, Xin R, Huang G, Liu Q. Effect of crystal orientation on the mechanical properties and strain hardening behavior of magnesium alloy AZ31 during uniaxial compression. Mater Sci Eng A 2012;534:588–93. doi:10.1016/j.msea.2011.12.013.

[16] Ma C, Chapuis A, Guo X, Zhao L, Wu P, Liu Q, et al. Modeling the deformation behavior of a rolled Mg alloy with the EVPSC-TDT model. Mater Sci Eng A 2017;682:332–40. doi:10.1016/j.msea.2016.11.027.

[17] Wang H, Raeisinia B, Wu PD, Agnew SR, Tomé CN. Evaluation of self-consistent polycrystal plasticity models for magnesium alloy AZ31B sheet. Int J Solids Struct 2010;47:2905–17. doi:10.1016/j.ijsolstr.2010.06.016.

[18] Hazeli K, Cuadra J, Vanniamparambil PA, Kontsos A. In situ identification of twin-related bands near yielding in a magnesium alloy. Scr Mater 2013;68:83–6. doi:10.1016/j.scriptamat.2012.09.009.

[19] Barnett MR, Nave MD, Ghaderi A. Yield point elongation due to twinning in a magnesium alloy. Acta Mater 2012;60:1433–43. doi:10.1016/j.actamat.2011.11.022.

[20] Wu PD, Guo XQ, Qiao H, Lloyd DJ. A constitutive model of twin nucleation, propagation and growth in magnesium crystals. Mater Sci Eng A 2015;625:140–5. doi:10.1016/j.msea.2014.11.096.

[21] Barnett MR. Twinning and the ductility of magnesium alloys. Mater Sci Eng A 2007;464:1–7. doi:10.1016/j.msea.2006.12.037.

[22] Hong S-G, Park SH, Lee CS. Role of {10–12} twinning characteristics in the deformation behavior of a polycrystalline magnesium alloy. Acta Mater 2010;58:5873–85. doi:10.1016/j.actamat.2010.07.002.

[23] Knezevic M, Levinson A, Harris R, Mishra RK, Doherty RD, Kalidindi SR. Deformation twinning in AZ31: Influence on strain hardening and texture evolution. Acta Mater 2010;58:6230–42. doi:10.1016/j.actamat.2010.07.041.

[24] WANG Z, CHAPUIS A, LIU Q. Simulation of mechanical behavior of AZ31 magnesium alloy during twin-dominated large plastic deformation. Trans Nonferrous Met Soc China 2015;25:3595–603. doi:10.1016/S1003-6326(15)64000-6.

[25] LOU X, LI M, BOGER R, AGNEW S, WAGONER R. Hardening evolution of AZ31B Mg sheet. Int J Plast 2007;23:44–86. doi:10.1016/j.ijplas.2006.03.005.

[26] Wang H, Wu PD, Tomé CN, Wang J. A constitutive model of twinning and detwinning for hexagonal close packed polycrystals. Mater Sci Eng A 2012;555:93–8. doi:10.1016/j.msea.2012.06.038.

[27] Chapuis A, Liu Q. Simulations of texture evolution for HCP metals: Influence of the main slip systems. Comput Mater Sci 2015;97:121–6. doi:10.1016/j.commatsci.2014.10.017.

[28] Barnett MR. Twinning and the ductility of magnesium alloys. Mater Sci Eng A 2007;464:8–16. doi:10.1016/j.msea.2007.02.109.

[29] Martin É, Capolungo L, Jiang L, Jonas JJ. Variant selection during secondary twinning in Mg–3%Al. Acta Mater 2010;58:3970–83. doi:10.1016/j.actamat.2010.03.027.

[30] Mu S, Jonas JJ, Gottstein G. Variant selection of primary, secondary and tertiary twins in a deformed Mg alloy. Acta Mater 2012;60:2043–53. doi:10.1016/j.actamat.2012.01.014.